LA-UR -92-149

LA-UR--92-149

DE92 007712

TITLE INTERMITTENCY GROWTH IN 3D TURBULENCE

AUTHOR(S) Y. KIMURA

SUBMITTED TO The Proceedings of the Workshop "Topological Fluid Dynamics" held in Santa Barbara, CA, November 1-5, 1991

To be published in the forthcoming book:

TOPOLOGICAL ASPECTS of the DYNAMICS of FLUIDS and PLASMAS
Proceedings of the Program of the Institute for Theoretical Physics, University of California at Santa Barbara (eds. H.K. Moffatt, G.M. Zaslavsky, M. Tabor & P. Comte). Kluwer Academic Publisher, Dordrecht, Netherlands.

INTERMITTENCY GROWTH IN 3D TURBULENCE

Y. KIMURA
Center for Nonlinear Studies
Los Alamos National Laboratory
Los Alamos, New Mexico 87545, U.S.A.

and

National Center for Atmospheric Research
P.O. Box 3000
Boulder, Colorado 80307, U.S.A.

1. Introduction

Recently increasing attention has been paid to the non-Gaussian properties of small scales in turbulent flows as a manifestation of intermittency.[1] Past numerical studies were, however, almost always restricted to simulations with external forces or to results after several eddy-turn-over times. This is because the equilibrium shapes of the Probability Density Functions (PDFs) of velocity and velocity gradients were the main concern (Kerr, 1985; Yamamoto and Hosokawa, 1988; She, Jackson and Orszag, 1988; Kida and Murakami, 1989; Métais and Herring, 1989; Vincent and Meneguzzi, 1991).

As a theoretical tool to analyze non-Gaussianity, Kraichnan and his co-workers developed a systematic technique called mapping closure. The working hypothesis of the technique is that the shape of PDF is determined by a balance between advection which produces active small eddies and dissipation which wipes them out. As these processes have different time scales (i.e., dissipation becomes effective later than advection for fields initially at large scales), different shapes of PDF are possible as a result of combinations of the processes. Accurate statistical calculations for decaying turbulence with the initial Gaussian distribution is vital, in the examination of the hypothesis.

[1] The reader is referred to a recent query about the prevalence of exponentials as non-Gaussian addressed by Narasimha and discussed by Herring in "*Whither Turbulence? Turbulence at the Crossroads*" ed. Lumley, J.L. (Springer, 1989).

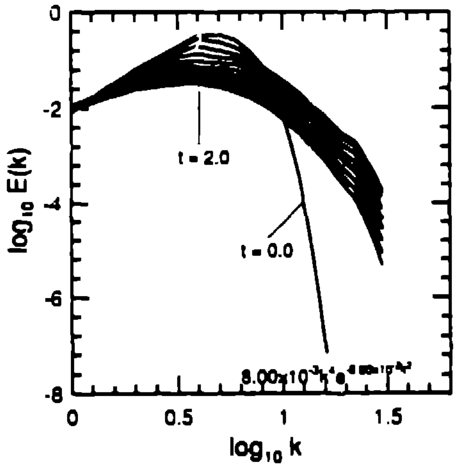

Fig. 1. Development of the kinetic energy spectrum. The initial spectrum is $E(k,0) = 0.008k^4 exp(-0.088k^2)$, and others are plotted with a time interval of 0.2 up to $t = 2.0$.

In this article, we shall present numerical results on the development of the shape of PDFs of the velocity components and transverse velocity gradients of Navier-Stokes turbulence (section 2). The possibility of controlling intermittency will be discussed in section 3. We used three-dimensional pseudospectral simulations with 64^3 periodic grid points. To get clean statistical information, averages over a large number of ensembles of different initial conditions satisfying the same energy spectrum were taken.

2. Numerical Results

First we shall see the time scale difference in various quantities such as developments of the energy spectrum, dissipation rate of energy, skewness factor of longitudinal velocity gradients, and kurtosis factor of transverse velocity gradients.

The development of the energy spectrum is shown in Fig.1. The initial spectrum is

$$E(k,0) = 0.008k^4 exp(-0.088k^2) \ . \tag{1}$$

and subsequent $E(k,t)$ are plotted with a time interval of 0.2 up to $t = 2.0$. (The time is not normalized by the eddy-turnover time of about 0.2.) The initial Taylor's microscale Reynolds number is about 40. The spectrum first changes to a self-similar stage and then decays uniformly, with the transition to self-similarity finished around $t \sim 0.4$.

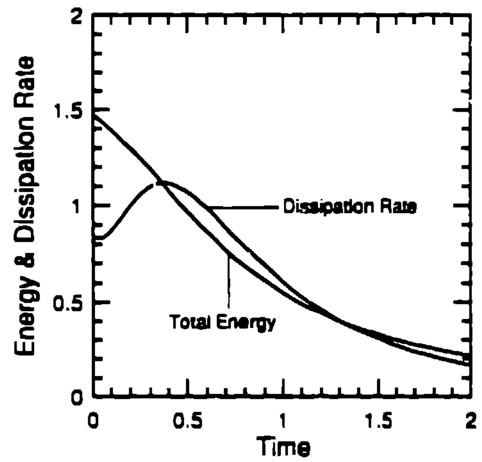

Fig. 2. The total kinetic energy $E_{tot} = \frac{1}{2}\sum_{\mathbf{k}}|\mathbf{v}(\mathbf{k})|^2$ and the energy dissipation rate, $\mathcal{E} = -\frac{d}{dt}E_{tot}$ as functions of time.

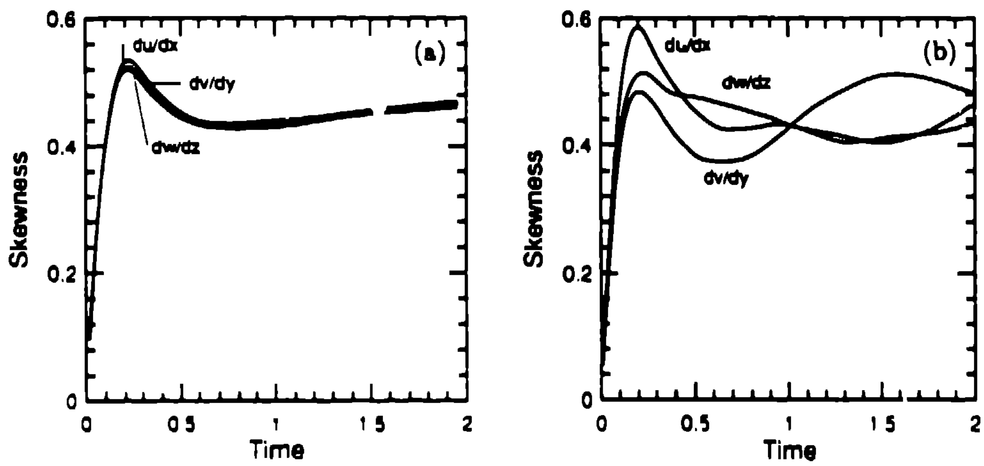

Fig. 3. The skewness factor of longitudinal velocity gradients. (a) ensemble average of 100 realizations; (b) single realization.

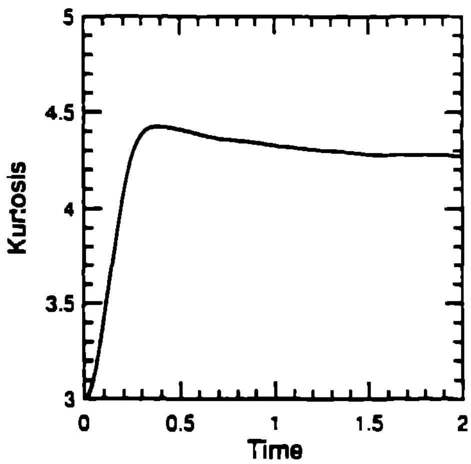

Fig. 4. The kurtosis factor of transverse velocity gradients.

In Fig. 2 we plot the total kinetic energy,

$$E_{tot} = \frac{1}{2}\sum_{\mathbf{k}} |\mathbf{v}(\mathbf{k})|^2 \ , \tag{2}$$

and the energy dissipation rate,

$$\mathcal{E}(t) = -\frac{d}{dt}E_{tot} \ , \tag{3}$$

as functions of time. The energy dissipation rate (which is proportional to the enstrophy for isotropic turbulence) has a maximum value at $t \sim 0.4$, and this time coincides with that of the appearance of the self-similar stage in the energy spectrum development.

The following relationship is known for the enstrophy D (Lesieur 1987),

$$\frac{dD}{dt} = \sqrt{\frac{98}{135}}S(t)D^{3/2} - 2\nu P(t) \ , \tag{4}$$

where $D(t)$ is the enstrophy,

$$D(t) \equiv \int_0^\infty k^2 E(k,t)dk \ , \tag{5}$$

$S(t)$ is the skewness factor of longitudinal velocity gradients,

$$S(t) = \frac{\langle(\partial u_i/\partial x_i)^3\rangle}{\langle(\partial u_i/\partial x_i)^2\rangle^{3/2}} \ , \quad (i = 1,2,3) \ , \tag{6}$$

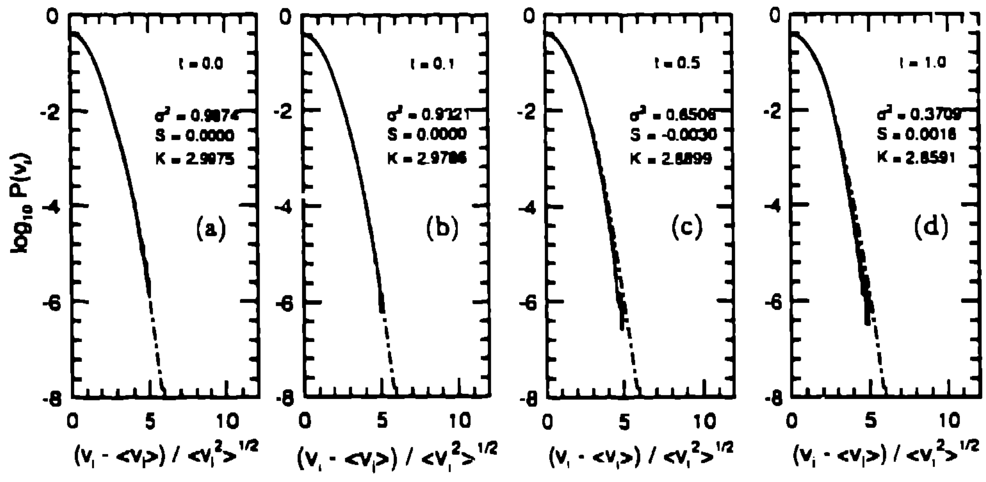

Fig. 5. PDFs of velocity components (a) t=0.0, (b) t=0.1, (c) t=0.5, (d) t=1.0.

(no summation rule is adopted), and $P(t)$ is the palinstrophy,

$$P(t) \equiv \int_0^\infty k^4 E(k,t) dk \quad . \tag{7}$$

The initial slight decrease in $\mathcal{E}(t)$ is due to the viscous term in (4) because $S(t)$ is zero for the Gaussian distribution. The nonlinear term then becomes gradually effective, and $\mathcal{E}(t)$ (or $D(t)$) increases until the viscous term begins to be dominant again because of the energy transfer to smaller scales.

If ν is 0 and $S(t)$ is positive (-definite), the enstrophy will blow up at a certain finite time, giving a real-time singularity for this case. When ν is not zero, on the other hand, the enstrophy will be de-singularized. and we might have a conjugate pair of complex-time singularities.

The skewness factor of the three longitudinal velocity gradients are plotted from the average of 100 realizations (a), and a single realization (b), in Fig. 3. The difference between (a) and (b) clearly shows that the ensemble average is needed to extract an isotropic feature of the skewness factor from the data to enable us to discuss a possible enstrophy blow-up by virtue of (4).

Figure 3 shows a sizable overshoot around $t \sim 0.22$, and a stable stage appears after that which agrees with the theoretical predictions (for example, the E.D Q.N.M. theory by André and Lesieur, 1977), and also with previous simulations (for example, Brachet *et al.*, 1983).

There is a time difference, albeit small, between the peak of the dissipation rate of energy and that of the skewness.[2] Intuitively speaking, $S(t)$ is

[2] This was pointed out by R.M. Kerr

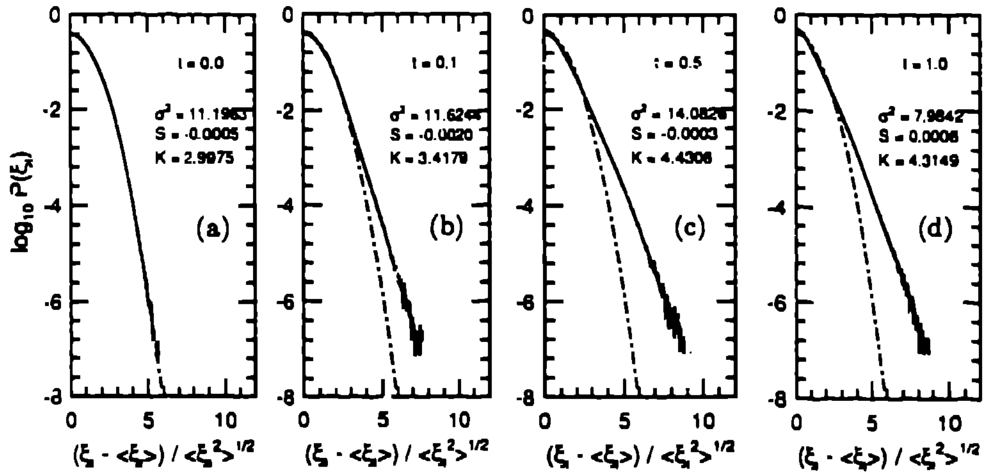

Fig. 6. PDFs of the transverse velocity gradients (a) t=0.0, (b) t=0.1, (c) t=0.5, (d) t=1.0.

an indicator of the energy transfer, and the enstrophy is produced by the energy transfer. Apparently, it seems natural that $S(t)$ (*cause*) has an earlier peak than $\mathcal{E}(t)$ (*effect*), but the true mechanism is still an unsolved problem.

Figure 4 shows the kurtosis factor of transverse velocity gradients $K(t)$,

$$K(t) \equiv \frac{\langle(\partial u_i/\partial x_j)^4\rangle}{\langle(\partial u_i/\partial x_j)^2\rangle^2} \ , \ \ (i \neq j : 1,2,3) \ , \tag{8}$$

which is another crucial quantity indicating a departure from Gaussianity, i.e., intermittency. The plot is an average kurtosis of 6 different kinds of transverse gradient, and each is obtained as an ensemble average of 10 realizations of initial conditions.

Starting from 3.0, characteristic for the Gaussian distribution, $K(t)$ increases rapidly and maximizes at $t \sim 0.4$, then decreases slowly to a stationary value. The time for the maximum kurtosis coincides with that for the dissipation rate, therefore the biggest (spatial) intermittency appears when the enstrophy becomes maximum. This suggests that if the maximum enstrophy is associated with a complex-time singularity so is the maximum kurtosis factor. Thus the coincidence of the peak times implies a crucial roll of complex-time singularities in spatial intermittency as well as in temporal intermittency, which was proposed a decade ago by Frisch and Morf (1981).

PDFs of velocity components and their transverse gradients are shown in Figs. 5 and 6. The data of the PDFs were sampled at $t = 0.0, 0.1, 0.5, 1.0$, and accumulated from 100 realizations. To get higher accuracy, we combined the three components of velocity and the six components of transverse gradients

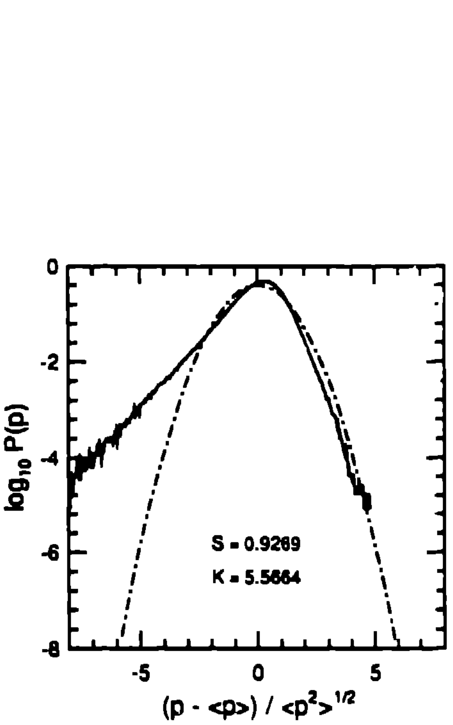

Fig. 7. PDFs of the pressure in Navier-Stokes turbulence.

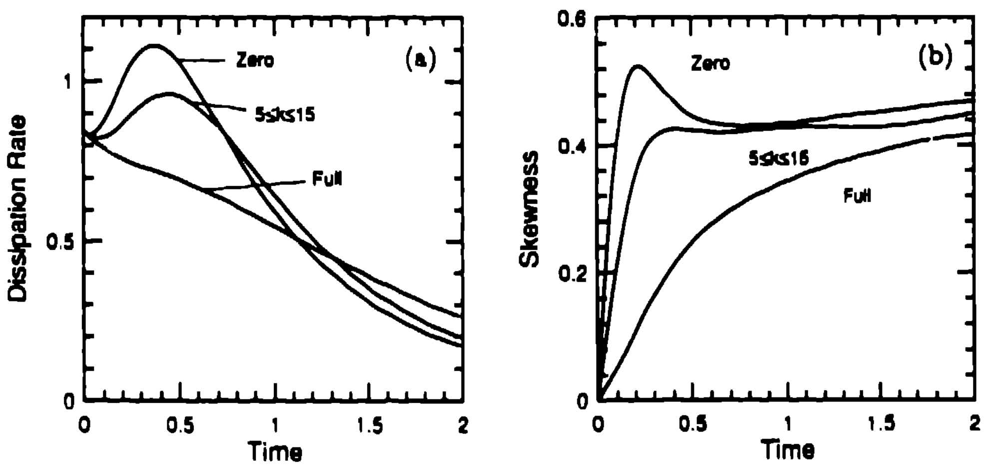

Fig. 8. Effect of helicity input on (a) the dissipation rate, and (b) the skewness factor of longitudinal velocity gradients. "Zero", "$5 \leq k \leq 15$", and "Full" mean the input of helicity in "no wave band (exactly zero helicity)", "a wave band of $5 \leq k \leq 15$", and "full wave band", respectively.

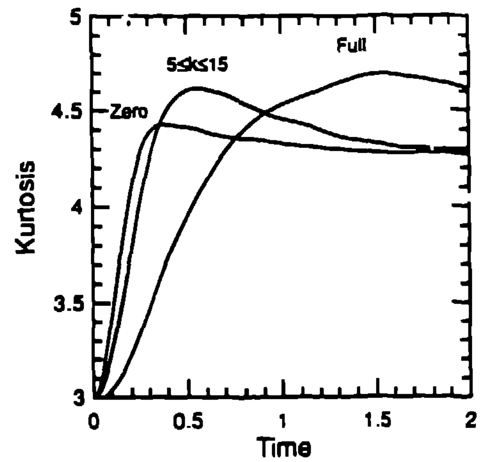

Fig. 9. Effect of helicity input on the kurtosis factor of transverse velocity gradients.

together, respectively, and folded at the vertical axis because both kinds of PDFs should be symmetric with this axis.

The PDFs of velocity components show thinner shapes than the Gaussian distribution (dashed line) in Fig. 5. This small inward defect from Gaussian was already reported in Fig. 4 of Vincent and Meneguzzi (1991). But they ignored this defect to conclude that the PDF of velocity components is close enough to Gaussian, which is well-known from many experiments (for example, Van Atta and Chen, 1968). The result in Fig. 5 suggests a reconsideration of the Gaussianity of velocity components in turbulence.[3]

The PDFs of transverse gradients show exponential-like tails, as already reported from both experiments (Van Atta and Chen, 1970; Castaing, Gagne and Hopfinger, 1990) and simulations (Yamamoto and Hosokawa, 1988; She, Jackson and Orszag, 1988; Kida and Murakami, 1989; Métais and Herring, 1989; Vincent and Meneguzzi, 1991) (Fig. 6). The departure from Gaussian is already saturated at $t = 0.5$. From Fig. 4, the saturation time seems to be $t \sim 0.4$ when $K(t)$ obtains the maximum value. Though some work has been done to elucidate the exponential-like tails (Kraichnan, 1991; She, 1991), treatment of non-local quantities like the pressure or its gradient remains open to conjecture. Figure 7 shows a typical PDF of the pressure of Navier-Stokes turbulence. The asymmetric feature of the pressure PDF has been

[3] In his text book (*The theory of homogeneous turbulence*, Cambridge University Press, 1953, p. 170), Batchelor cited an experimental result by R.W. Stewart on the kurtosis factor of velocity difference. When a spatial distance is large, two velocities are statistically independent and the kurtosis factor is reduced to $\frac{3}{2} + \frac{\langle u_1^4 \rangle}{2\langle u_1^2 \rangle^2}$. Stewart's plot shows a lower value than 3 asymptotically, which indicates a lower kurtosis for velocity components.

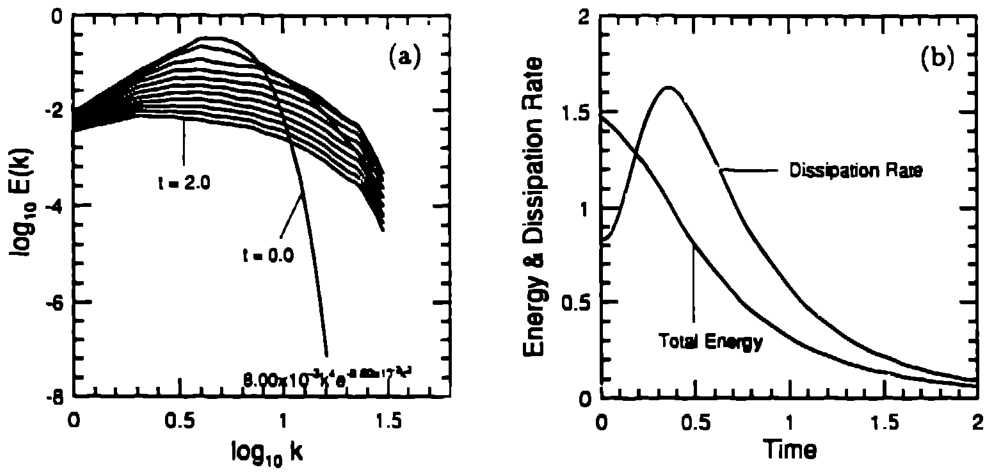

Fig. 10. (a) The energy spectra for the passive-vector equation under a frozen random advecting velocity; (b) the dissipation rate of energy.

already observed (for isotropic turbulence, Métais and Lesieur, 1991; for a mixing layer, Comte, Lesieur and Lamballais, 1991), and this may play an important role in clarifying the mechanism of the intermittency growth.

3. Control of intermittency

We have seen that the developments of PDFs are intimately related to the balance between advection and dissipation in turbulence. Thus intermittency might be controllable if we can somehow adjust the balance. In order to adjust the balance we propose two heuristic numerical methods. One would input the helicity initially and the other would modify the Navier-Stokes equation.

3.1. INITIAL HELICITY INPUT

Helicity is a conservative quantity for an inviscid flow which measures the degree of knottedness of the vortex lines (Moffatt, 1969). As was suggested by Kraichnan (1973), the helicity (or the partial alignment of velocity **u** with vorticity $\boldsymbol{\omega}$) reduces the effect of the nonlinearity $\mathbf{u} \times \boldsymbol{\omega}$ and depresses the overall turbulent energy transfer. When a flow is viscous, the helicity itself decays, and the decay rate of the ratio of the total helicity and the total energy plays an important role. If the helicity can be sustained until the peak time of enstrophy, there seems to be a significant effect on vortex stretching.

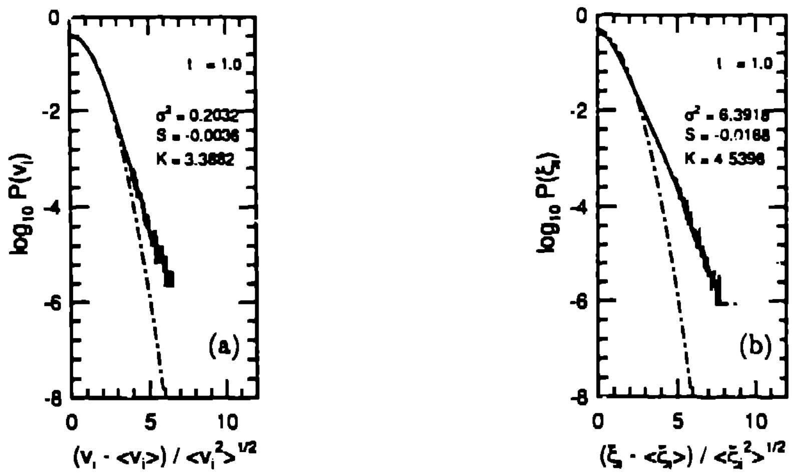

Fig. 11. PDFs of (a) the components and (b) the transverse gradients, of **u** (passive vector equation). They both show exponential-like non-Gaussian tails.

Helicity H in the k-space expression is

$$H = \sum_{\mathbf{k}} \mathbf{u}(\mathbf{k}).\omega(-\mathbf{k}) = 2\sum_{\mathbf{k}} \mathbf{k}.[\mathbf{u}_r(\mathbf{k}) \times \mathbf{u}_i(\mathbf{k})] \ , \tag{9}$$

where $\mathbf{u}(\mathbf{k}) = \mathbf{u}_r(\mathbf{k}) + i\mathbf{u}_i(\mathbf{k})$ (Polifke, 1991). Thus, by adjusting the angles between the real and imaginary vectors of complex velocities in the wave space, we can input the helicity to the wave modes. To maintain the incompressibility, first a set of real vectors is generated such that each vector is perpendicular to a wave vector and is properly scaled for the energy spectrum. Then an imaginary vector, also perpendicular to the wave vector, is formed making a given angle with the real vector.

Figures 8a and 8b show the enstrophy and the skewness factor under three different initial values of helicity. We observed that the peaks of the enstrophy and the skewness factor became lower and shifted downward with the helicity input. The vortex stretching was eventually delayed and depressed. In Fig. 9, the corresponding kurtosis factors are plotted. Though the kurtosis factor was depressed at an early stage of development, it achieved a higher value as a greater helicity was input initially. The result seems paradoxical because the helicity which was supposed to suppress generation of small scales on the contrary enhanced intermittency. Further careful consideration of the generation of (helical) structures is necessary by checking other types of initial conditions (for example, anisotropic, or structured), or by changing the Reynolds number.

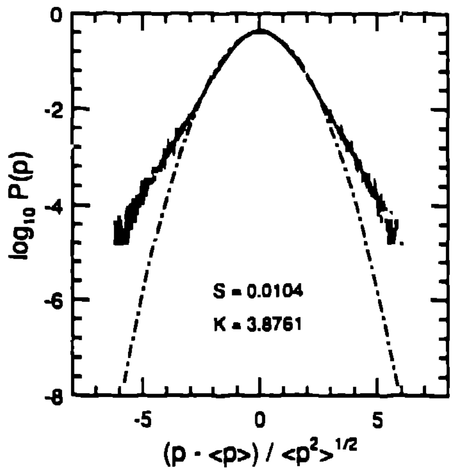

Fig. 12. PDFs of the pressure in the incompressible passive vector equation.

3.2. MODIFIED NAVIER-STOKES EQUATION

As a tool to analyze the intermittency growth in Navier-Stokes turbulence, we propose to study the following modified Navier-Stokes equation,

$$\frac{\partial \mathbf{u}}{\partial t} + (\mathbf{v}.\nabla).\mathbf{u} = -\alpha \nabla p + \nu \nabla^2 \mathbf{u} \ , \tag{10}$$

$$\nabla.\mathbf{v} = 0 \ . \tag{11}$$

The points of modification are summarized as follows:

- 1. The advecting velocity ($\mathbf{v}$) and the advected velocity ($\mathbf{u}$) are separated. We have a variety of choices for $\mathbf{v}$, such as,
  (i) frozen velocity field in time,
    (a) independent of $\mathbf{u}$ (random mixing),
    (b) initial field of $\mathbf{u}(0)$,
  (ii) refreshed after a period Δt (white noise approximation when $\Delta t \to 0$),
  (iii) velocity field governed by other equations.
- 2. A prefactor α is put before the pressure term,
  (i) $\alpha = 0$ (passive-vector equation),
  (ii) $\alpha = 1$ (incompressible passive-vector equation).

Here we concentrated only on cases in which $\mathbf{v}$ is frozen and independent of $\mathbf{u}$. (A detailed report is to be published soon, Kimura and Kraichnan.) Figures 10a and 10b plot the energy spectra and the dissipation rate of energy, respectively, when $\alpha = 0$ (passive vector equation). An obvious difference from those in the Navier-Stokes equation is that the slope of the middle wave-range is less steep. In accordance with the observation about the energy spectrum, which suggests a bigger energy transfer from large to small scales, the dissipation rate of energy shows a higher hump than the previous case. In contrast with the Navier-Stokes turbulence, however, the PDF of the components of **u** shows a much wider tail than in the Gaussian distribution (Fig. 11a), and the PDF of the transverse gradients attains even greater non-Gaussianity (Fig. 11b). The non-Gaussianity of the passive-vector equation as well as the passive-scalar equation are from a higher order effect because the Gaussian distribution should be expected when there is either only advection or diffusion. Research on the non-Gaussian distribution is still underway. As an example in which $\alpha = 1$ (incompressible passive vector equation), we raise the PDF of the pressure in Fig. 12. The most significant discrepancy from Fig. 7 is that the shape is symmetric, which may manifest a different mechanism in producing different intermittency.

Acknowledgements

Most of the present work is the result of collaboration with Bob Kraichnan. The author expresses his cordial thanks for his encouragement and discussions. The pseudo-spectral code was originally developed by R. Panda (IBM), and all calculations were done on a IBM 3090-300E with vector processors at Los Alamos National Laboratory. Special thanks go to C. Whittaker (IBM) for the computation. The author also thanks J. R. Herring, R. M. Kerr, D. Montgomery, and R. Pelz for fruitful suggestions, and the participants in the workshop on Topological Fluid Dynamics at the Institute for Theoretical Physics at the University of California, Santa Barbara, which is supported by NSF Grant PHY89-04035.

NCAR is sponsored by the National Science Foundation.

References

André, J.C. & Lesieur, M., 1977 Influence of helicity on high Reynolds number isotropic turbulence. *J. Fluid Mech.*, **81**, pp. 187-207

Brachet, M., Meiron, D.I., Orszag, S.A., Nickel, B.G., Morf, R.H. & Frisch, U., 1983 Small-scale structure of the Taylor-Green vortex. *J. Fluid Mech.*, **130**, pp. 411-452.

Castaing, B., Gagne, Y. & Hopfinger, E.J., 1990 Velocity probability density functions of high Reynolds number turbulence. *Physica*, **D 46**, pp. 177-200

Chen, H., Chen, S. & Kraichnan, R.H., 1989 Probability distribution of a stochastically advected scalar field. *Phys. Rev. Lett.*, **63**, pp. 2657-2660

Comte, P., Lesieur, M. & Lamballais, E., 1991 Large and small-scale stirring of vorticity and a passive scaler in a 3D temporal mixing layer. *Phys. Fluids*, **A**, submitted

Frisch, U. & Morf, R., 1981 Intermittency in nonlinear dynamics and singularities at complex times. *Phys. Rev.*, **A23**, pp. 2673-2705

KERR, R., 1985 Higher-order derivative correlations and the alignment of small-scale structures in isotropic numerical turbulence. *J. Fluid Mech.*, **153**, pp 31-58.

KIDA, S. & MURAKAMI, Y., 1989 Statistics of velocity gradients in turbulence at moderate Reynolds numbers. *Fluid Dyn. Res.*, 4, pp. 347-370.

KIMURA, Y. & KRAICHNAN, R.H., in preparation.

KRAICHNAN, R.H., 1973 Helical turbulence and absolute equilibrium *J. Fluid Mech.*, **59**, pp. 745-752.

KRAICHNAN, R.H., 1991 Turbulent cascade and intermittency growth. *Proc. R. Soc. London*, Turbulence and stochastic processes: Kolmogorov's ideas 50 years on. Eds. J.C.R. Hunt, O.M.Phillips and D. Williams, **A 434**, pp. 65-78.

LESIEUR, M., 1987 Turbulence in Fluids *Kluwer Academic Publishers*, p. 93.

MÉTAIS, O. & HERRING, J.R., 1989 Numerical studies of freely decaying homogeneous stratified turbulence. *J. Fluid Mech.*, **202**, pp. 117-148.

MÉTAIS, O. & LESIEUR, M., 1991 Spectral large-eddy simulation of isotropic and stably-stratified turbulence. *J. Fluid Mech.*, submitted.

MOFFATT, H.K., 1969 The degree of knottedness of tangled vortex lines. *J. Fluid Mech.*, **35**, pp. 117-129.

POLIFKE, W., 1991 Statistics of helicity fluctuations in homogeneous turbulence. *Phys. Fluids*, **A3**, pp. 115-129.

SHE, Z.-S., 1991 Physical model of intermittency in turbulence: Near-dissipation-range non-Gaussian statistics *Phys. Rev. Lett.*, **66**, pp. 600-603.

SHE, Z.-S., JACKSON, E. & ORSZAG, S.A., 1988 Scale-dependent intermittency and coherence in turbulence. *J. Sci. Comp.*, **3**, pp. 407-434.

VAN ATTA, C.W. & CHEN, W.Y., 1968 Correlation measurements in grid turbulence using digital harmonic analysis. *J. Fluid Mech.*, **34**, pp. 497-515.

VAN ATTA, C.W. & CHEN, W.Y., 1970 Structure functions of turbulence in the atmospheric boundary layer over the ocean. *J. Fluid Mech.*, **44**, pp. 145-159.

VINCENT, A. & MENEGUZZI, M., 1991 The spatial structure and statistical properties of homogenous turbulence. *J. Fluid Mech.*, **225**, pp. 1-20.

YAMAMOTO, K. & HOSOKAWA, I., 1988 A decaying isotropic turbulence pursued by the spectral method, *J. Phys. Soc. Japan*, **57**, pp. 1532-1535.